Magnetic Resonance Imaging (MRI): principles, applications and challenges

Università di Catania

CELEBRATING DR. MARCELLO BALDO'S 80TH BIRTHDAY
Catania, 16-17 October 2023

Giuseppe Stella

Associate Professor of Applied Physics [FIS/07]

Department of Physics and Astronomy "E. Majorana"

From NMR to MRI – Brief history

Nuclear magnetic resonance (NMR) is the spectroscopic study of the magnetic properties of the *nucleus* of the atom.

> ***Resonance*** *is the process in which nuclei subjected to a strong magnetic field selectively absorb and release their own energy and that of their environment*

In the early 1970s, it was realized that magnetic field gradients could be used to localize the NMR signal and to generate images that display magnetic properties of the proton, reflecting clinically relevant information, coupled with technological advances and development of "body-size" magnets.

As clinical imaging applications increased **in the mid-1980s** and the concept of **magnetic resonance imaging (MRI)**, became commonly accepted in the medical community.

Marcello Baldo's research

J. CHEM. SOC. PERKIN TRANS. II 1985

955

Molecular Determinants for Drug–Receptor Interactions. Part 5.† Anisotropic and Internal Motions in Analgesic Narcotics (Morphine, Oxymorphone) and Related Antagonists (Nalorphine, Naloxone) by Carbon-13 Nuclear Magnetic Resonance Spin–Lattice Relaxation Times

Giuseppe C. Pappalardo*
Istituto Dipartimentale di Chimica, II Cattedra di Chimica Generale, Facoltà di Farmacia, Università di Catania, Viale A. Doria 8, 95125 Catania, Italy
Lajos Radics
Central Research Institute for Chemistry, P.O. Box 17, H-1525 Budapest, Hungary
Marcello Baldo
INFN, Istituto Dipartimentale di Fisica, Università di Catania, Corso Italia 58, 95124 Catania, Italy
Antonio Grassi
Istituto Dipartimentale di Chimica, Cattedra di Chimica Generale, Facoltà di Farmacia, Università di Catania, Viale A. Doria 8, 95125 Catania, Italy

Spectrochimica Acta, Vol. 38A, No. 12, pp. 1253–1255, 1982
Printed in Great Britain.

A carbon-13 NMR spin-lattice relaxation study of the molecular conformation of the nootropic drug 2-oxopyrrolidin-1-ylacetamide*

M. BALDO, A. GRASSI, L. GUIDONI, M. NICOLINI, G. C. PAPPALARDO† and V. VITI

0584-8539/82/121253-03$03.00/0

Physica 114A (1982) 88–94 North-Holland Publishing Co.

BROWNIAN MOTION IN GROUP MANIFOLDS: APPLICATION TO SPIN RELAXATION IN MOLECULES

Marcello BALDO
Istituto Nazionale di Fisica Nucleare, Corso Italia 57, I-95129 Catania, Italy

Study of Carbon-13 NMR spin lattice relaxation time for investigate details of molecular motion in solution.

MAGNETIC RESONANCE PROPERTIES OF MEDICALLY USEFUL NUCLEI

NUCLEUS	SPIN QUANTUM NUMBER	% ISOTOPIC ABUNDANCE	MAGNETIC MOMENT[b]	% RELATIVE ELEMENTAL ABUNDANCE[a]	RELATIVE SENSITIVITY
^{1}H	½	99.98	2.79	10	1
^{3}He	½	0.00014	−2.13	0	–
^{13}C	−½	0.011	0.70	18	–
^{17}O	5/2	0.04	−1.89	65	9×10^{-6}
^{19}F	½	100	2.63	<0.01	3×10^{-8}
^{23}Na	3/2	100	2.22	0.1	1×10^{-4}
^{31}P	½	100	1.13	1.2	6×10^{-5}

[a]moment in nuclear magneton units = 5.05×10^{-27} J T^{-1}.
[b]*Note:* by mass in the human body (all isotopes).

Magnetic Characteristics of the Proton

When placed in a strong static magnetic field, B0, magnetic forces cause the protons to align with the applied field in parallel and antiparallel directions at two discrete energy levels.

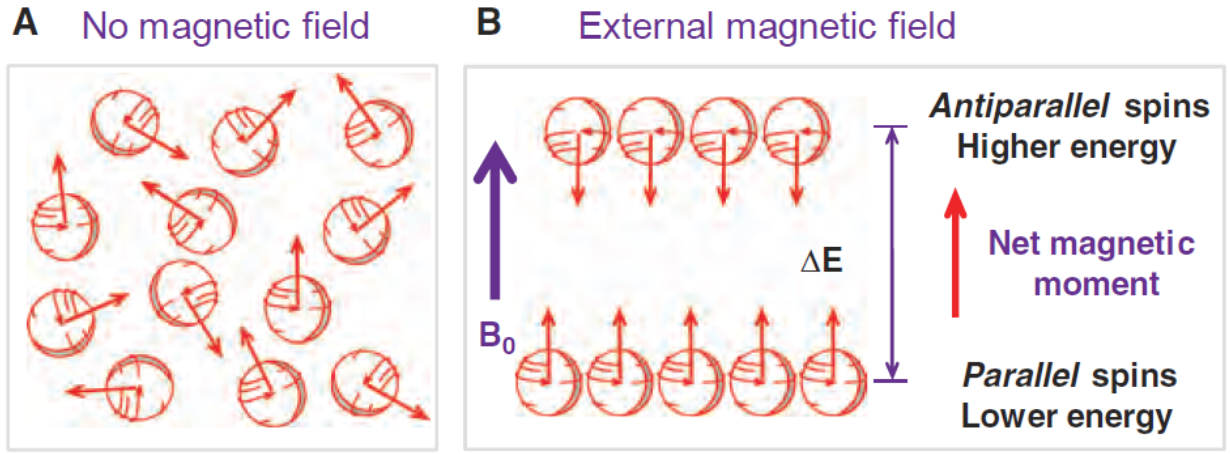

The protons also experience a torque in a perpendicular direction from the applied magnetic field that causes precession

The *Larmor equation* describes the dependence between the magnetic field, B_0, and the angular precessional frequency, ω_0:

$$\omega_0 = \gamma B_0$$

where g is the gyromagnetic ratio unique to each element. This is expressed in terms of linear frequency as where $\omega=2\pi f$ and $\gamma/2\pi$ is the *gyromagnetic ratio*, with values expressed in millions of cycles per second (MHz) per Tesla, or MHz/T.

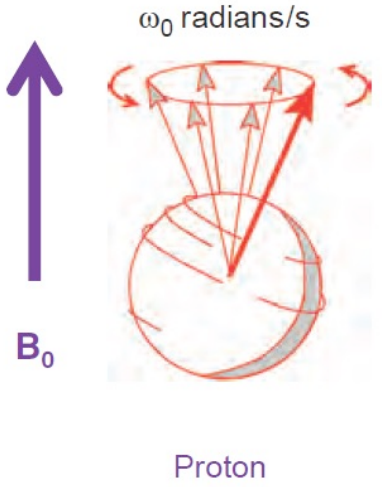

Energy Absorption and Emission

The protons precessing in the parallel and antiparallel directions result in a quantized distribution (two discrete energies) with the **NET MAGNETIC MOMENT** of the sample at equilibrium equal to the vector sum of the individual magnetic moments in the direction of B_0

NO measurable!

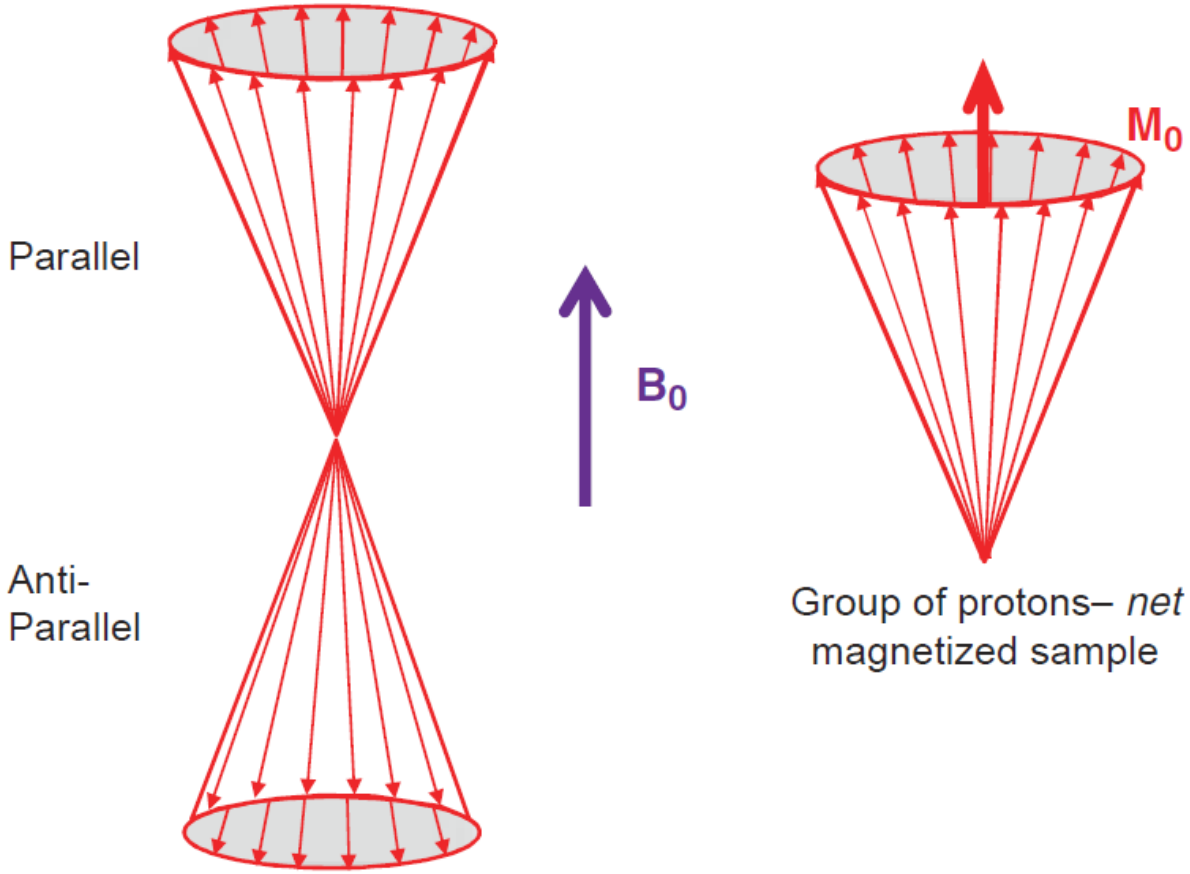

The Magnetic Resonance Signal

- Application of RF energy (from 0.3 to 4.0 T; 42.58 MHz/T) synchronized to the precessional frequency of the protons causes absorption of energy and displacement of the sample magnetic moment from equilibrium conditions
- The return to equilibrium results in the emission of energy proportional to the number of excited protons in the volume
- This occurs at a rate that depends on the structural and magnetic characteristics of the sample.
- Excitation, detection, and acquisition of the signals constitute the basic information necessary for **MRI**.

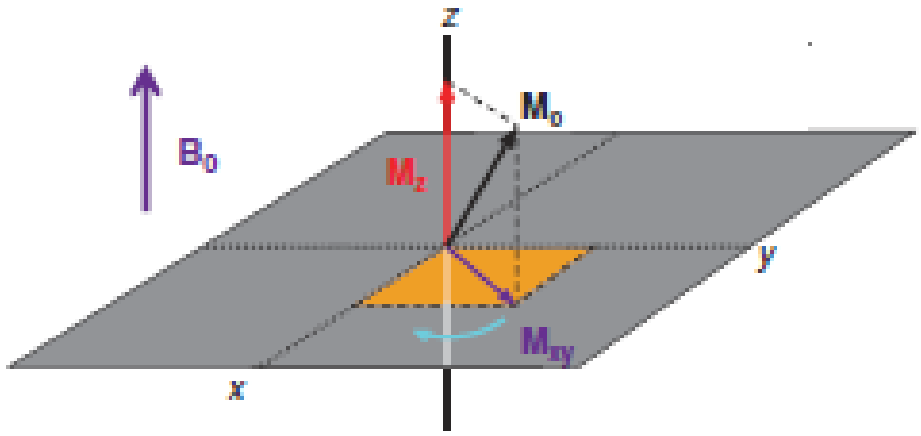

Magnetization Properties of Tissues - T2 Relaxation

After a 90-degree RF pulse is applied to a magnetized sample at the Larmor frequency, an initial phase coherence of the individual protons is established and maximum M_{xy} is achieved.

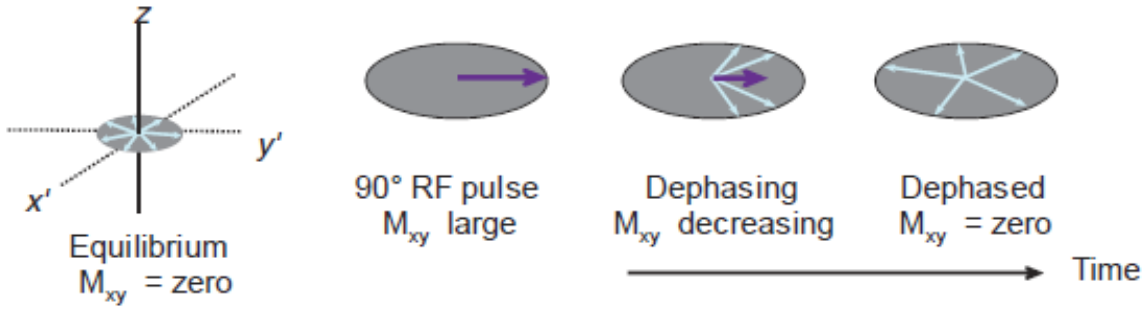

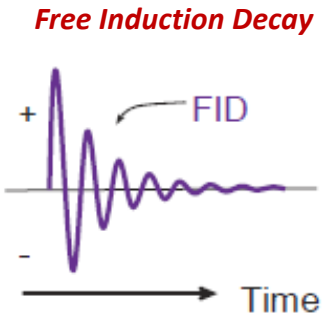

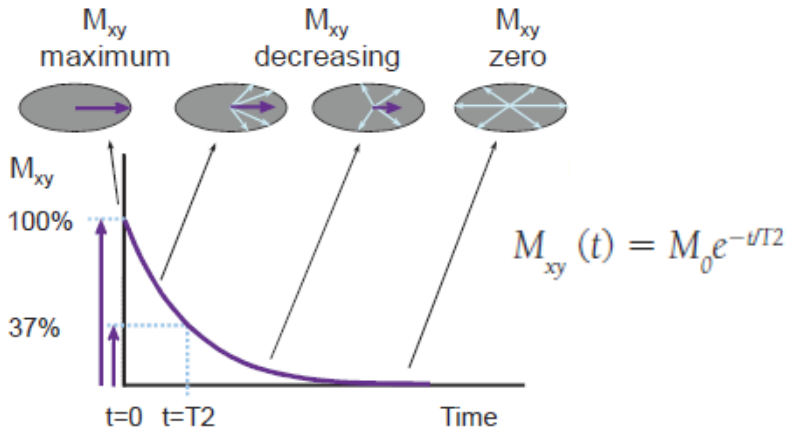

Extrinsic magnetic inhomogeneities, such as the imperfect main magnetic field, B_0, or susceptibility agents in the tissues (e.g., MR contrast materials, paramagnetic or ferromagnetic objects), add to the loss of phase coherence from intrinsic inhomogeneities and further reduce the decay constant, known as T2* under these conditions

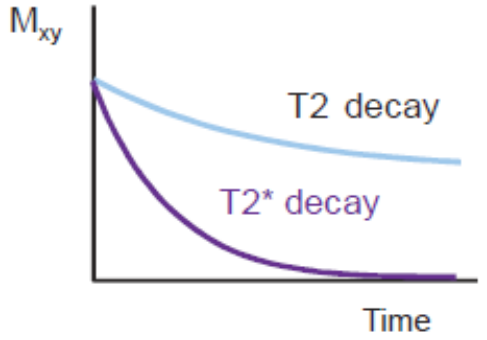

Magnetization Properties of Tissues – T1 Relaxation

Longitudinal magnetization begins to recover immediately after the B_1 excitation pulse, simultaneous with transverse decay

Spin-lattice relaxation is the term describing the release of energy back to the lattice, and the regrowth of M_z

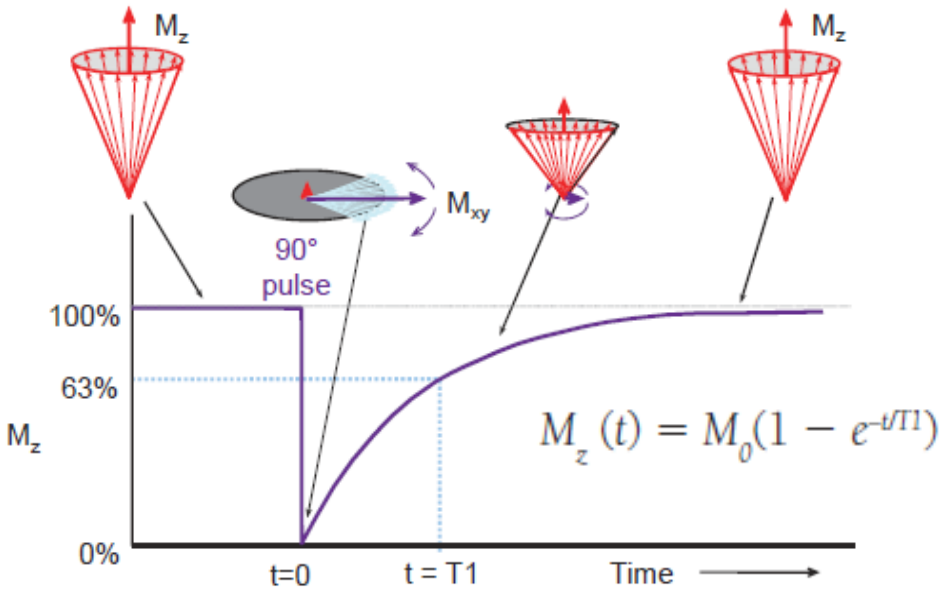

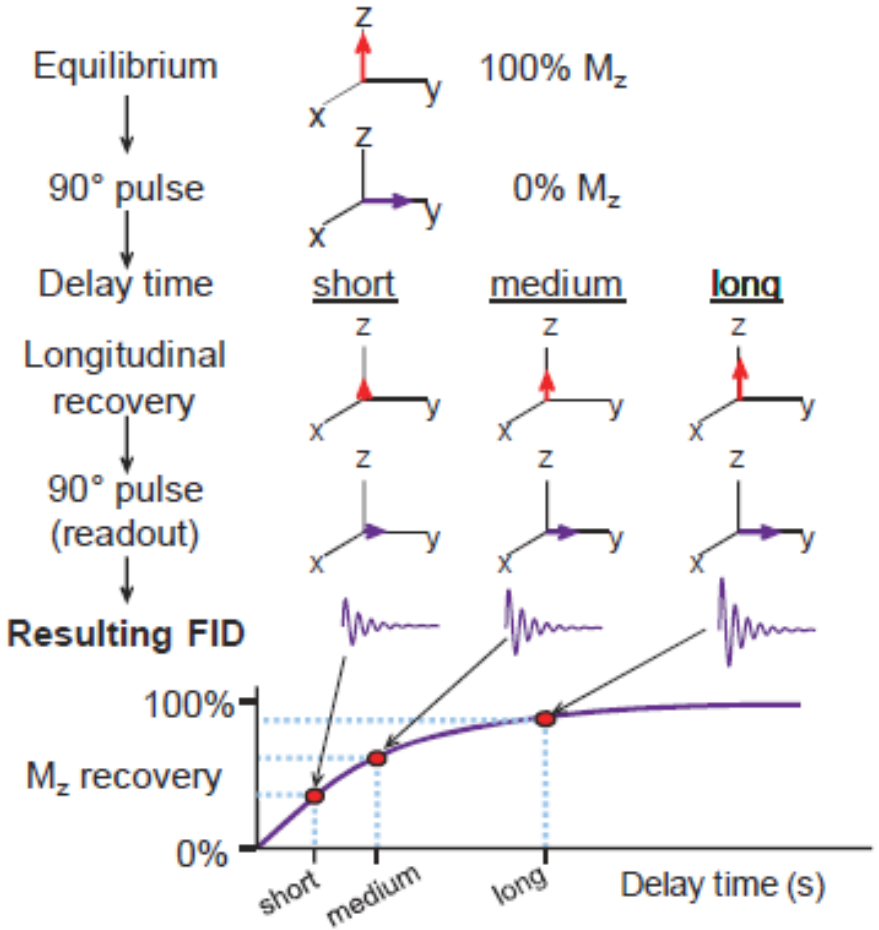

After a 90-degree pulse, M_z is converted from a maximum value at equilibrium to $M_z = 0$.

Return of M_z to equilibrium occurs exponentially and is characterized by the spin-lattice T1 relaxation constant.

Comparison of T1 and T2

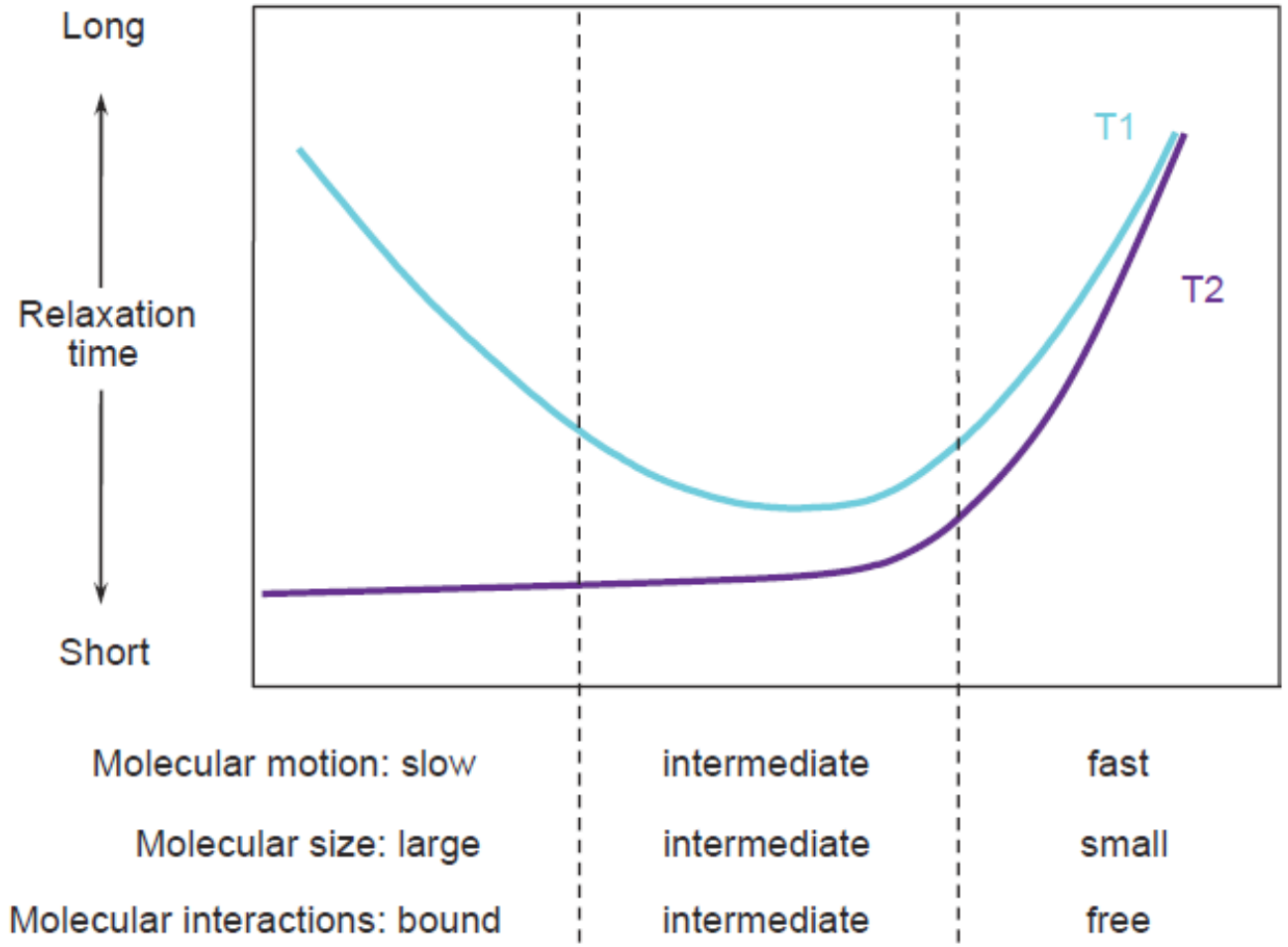

- Factors affecting T1 and T2 relaxation times of different tissues are generally based on molecular motion, size, and interactions that have an impact on the local magnetic field variations (T2 decay) and structure with intrinsic tumbling frequencies coupling to the Larmor frequency (T1 recovery).

- The relaxation times (vertical axis) are different for T1 and T2.

Basic Acquisition Parameters

Time of Repetition

- The time of repetition (TR) is the period between B_1 excitation pulses.
- During the TR interval, T2 decay and T1 recovery occur in the tissues.
- TR values range from extremely short (ms) to extremely long (10,000 ms) time periods, determined by the type of sequence employed.

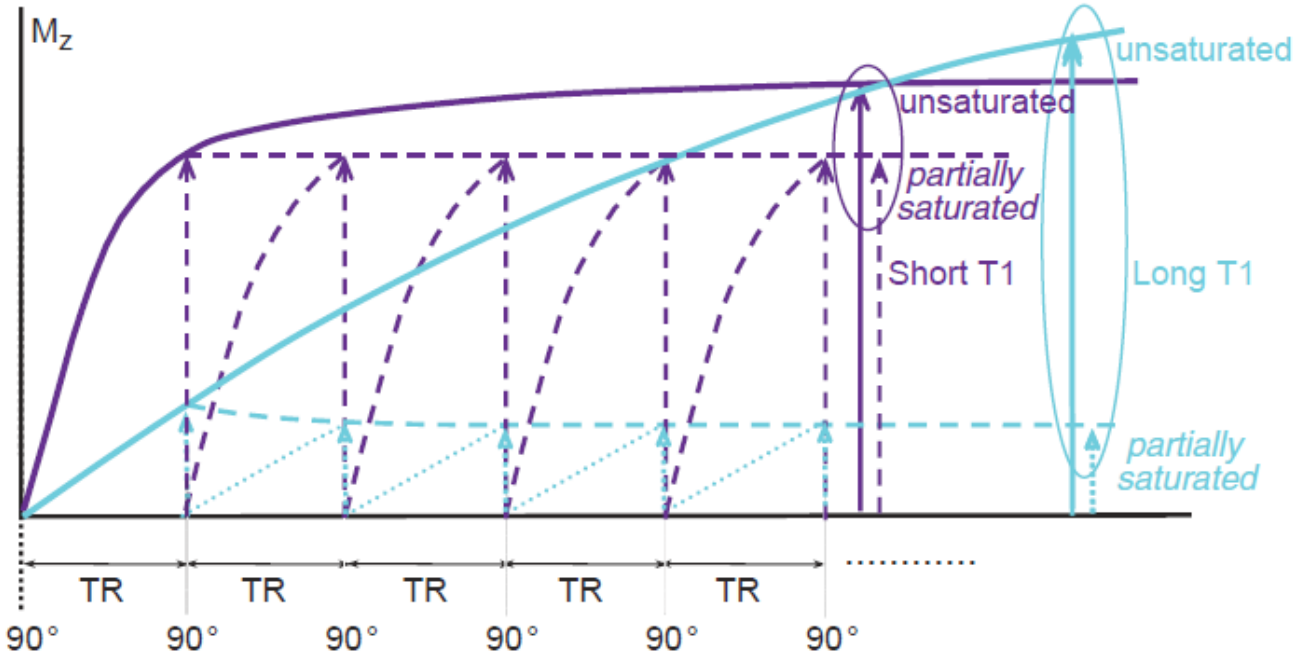

- First pulse: Partial saturation of tissues occurs because the repetition time between excitation pulses does not allow for full return to equilibrium.
- Second pulse: the M_z amplitude for the next RF pulse is reduced.
- Third pulse: a steady-state equilibrium is reached, where the amount of longitudinal magnetization is the same from pulse to pulse, as is the transverse magnetization for a tissue with a specific T1 decay constant.
- Tissues with long T1 experience a greater partial saturation than do tissues with short T1 as shown above. Partial saturation is important in understanding contrast mechanisms and signal from unsaturated and saturated tissues.

Basic Acquisition Parameters

Time of Echo

To separate the RF energy deposition and returning signal, an “echo” is induced to appear at a later time, with the application of a 180-degree RF inversion pulse.

The time of echo (TE) is the time between the excitation pulse and the appearance of the peak amplitude of an induced echo, which is determined by applying a 180-degree RF inversion pulse or gradient polarity reversal at a time equal to TE/2.

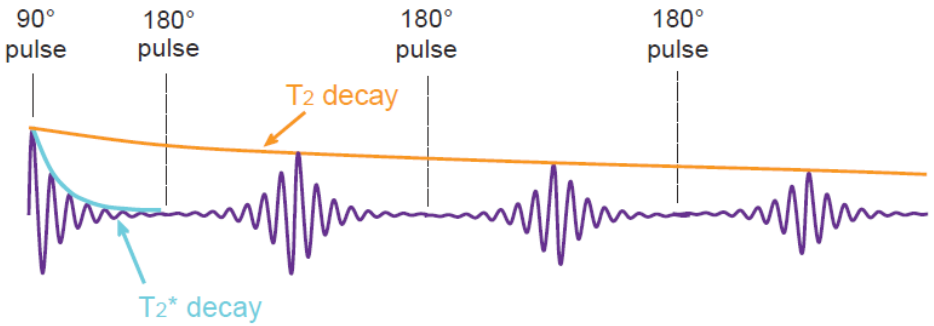

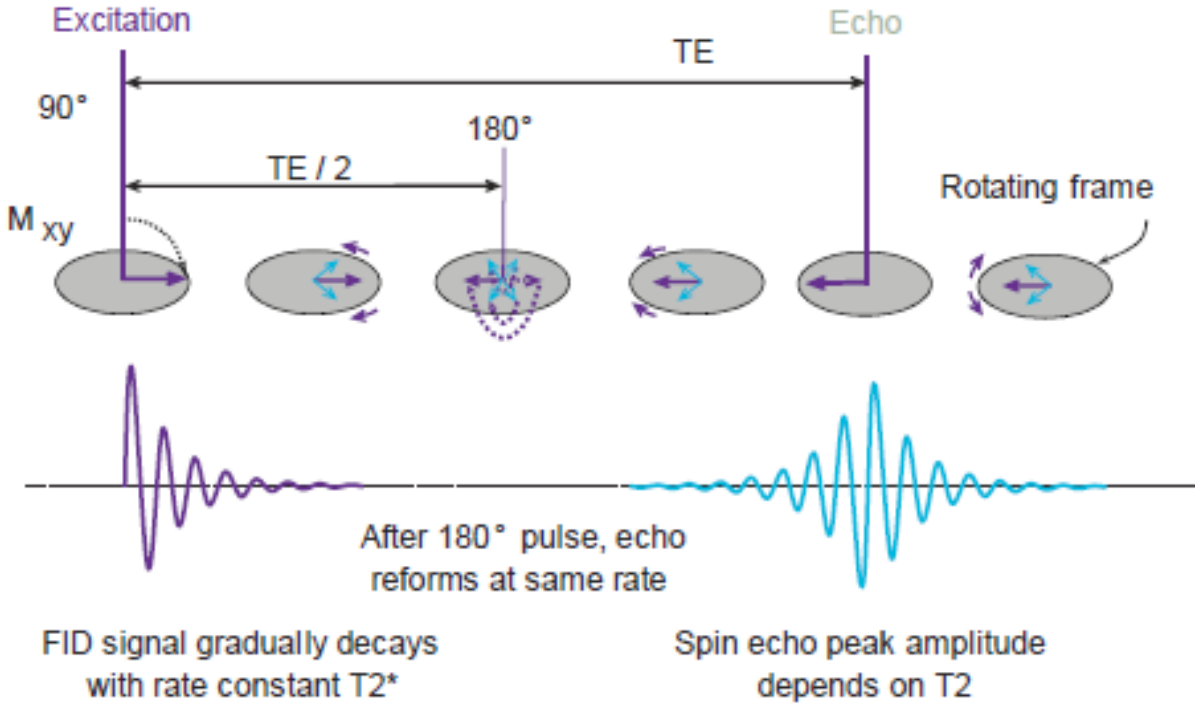

- “True” T2 decay is determined from multiple 180-degree refocusing pulses acquired during the repetition period.
- FID envelope decays with the T2* decay constant
- The peak amplitudes of subsequent echoes decay exponentially according to the T2 decay constant (magnetic field inhomogeneities are cancelled)

$$S \propto r_H \left[1 - e^{TR/T1}\right] e^{-TE/T2}$$

T1-weighted contrast

Brain tissues

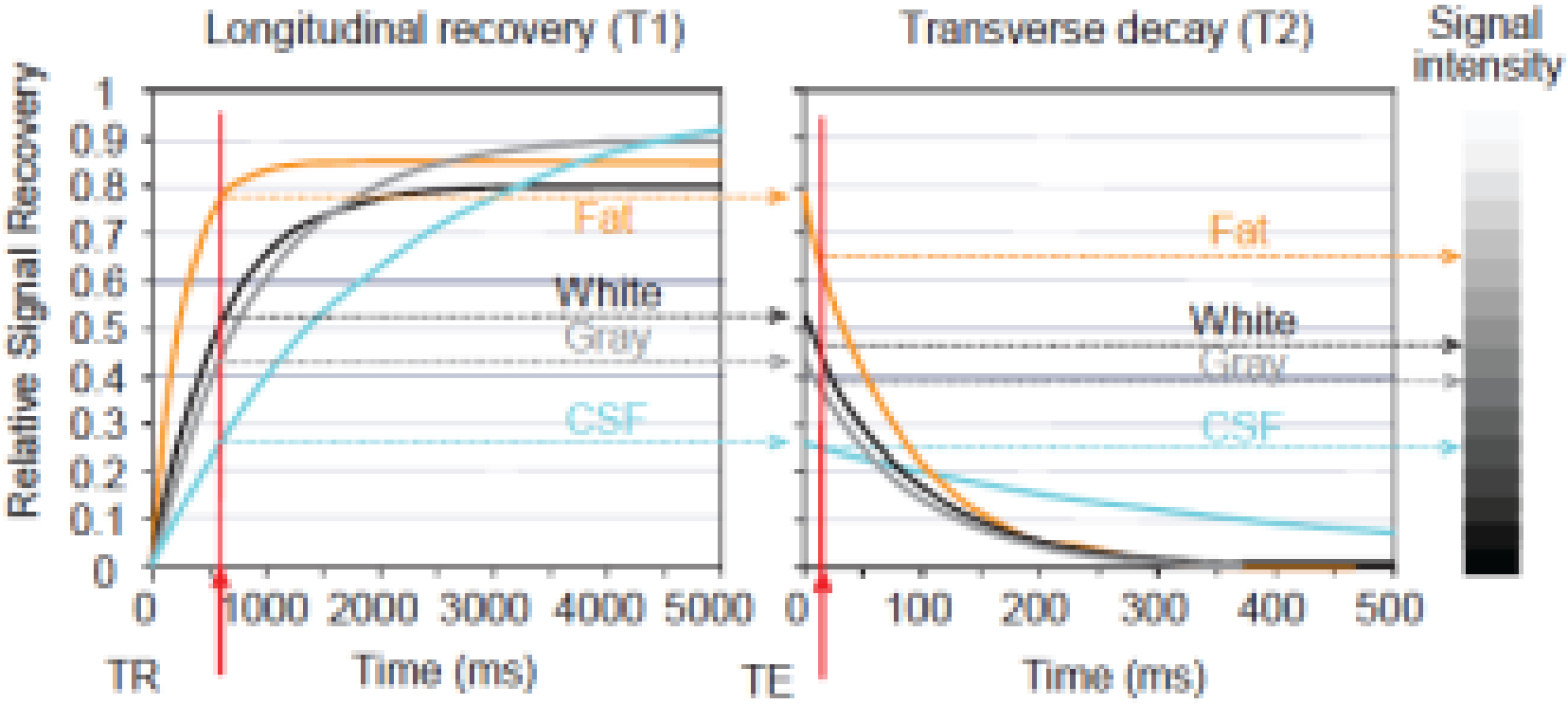

T1-weighted contrast requires the selection of a TR that emphasizes the differences in the T1 characteristics of the tissues (e.g., TR = , 500 *ms*), and reduces the T2 characteristics by using a short TE so that transverse decay is reduced (e.g., TE <= 15 *ms*).

Proton density weighting

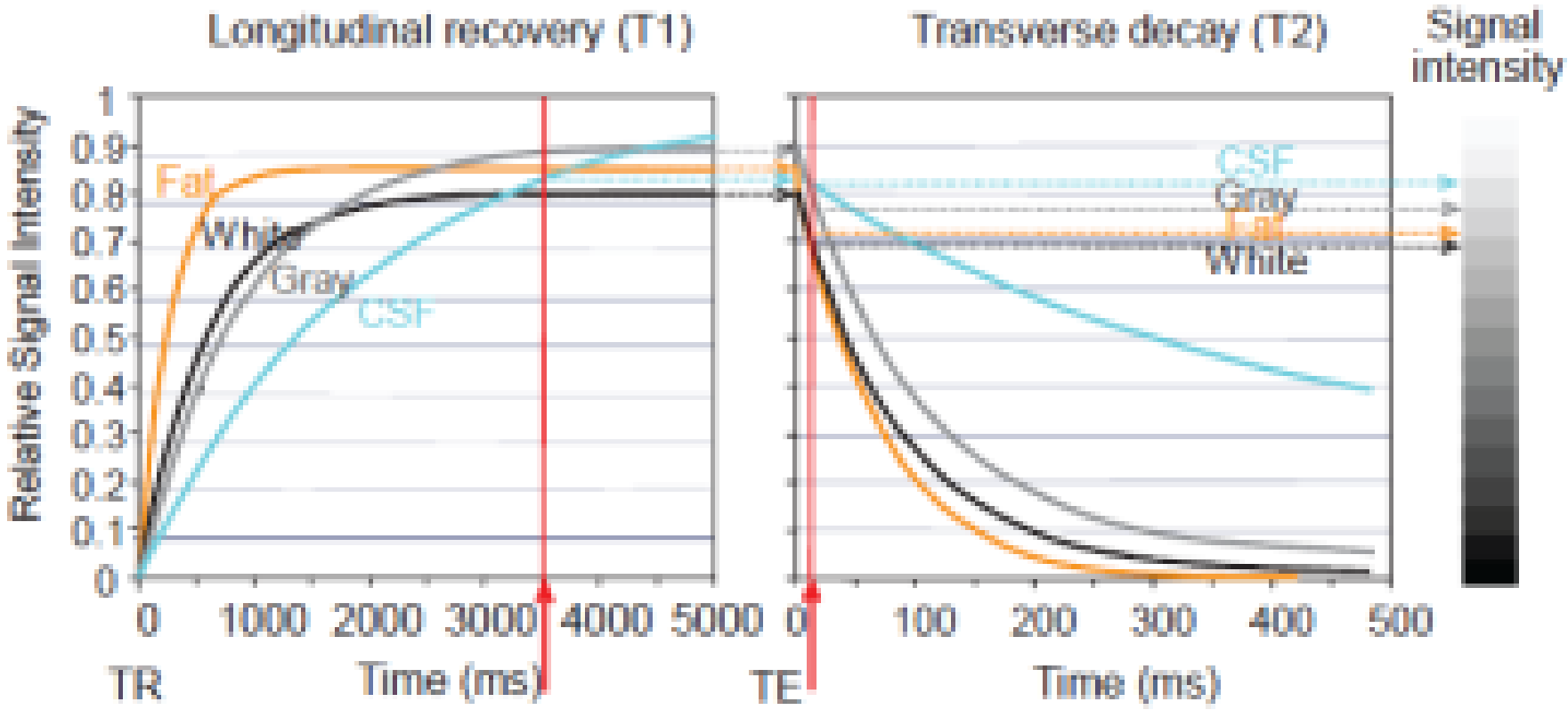

Proton (spin) density weighted contrast requires the use of a long TR (e.g., greater than 2,000 *ms*) to reduce T1 effects, and a short TE (e.g., less than 35 *ms*) to reduce T2 influence in the acquired signals. Note that the average overall signal intensity is higher.

T2 weighted contrast

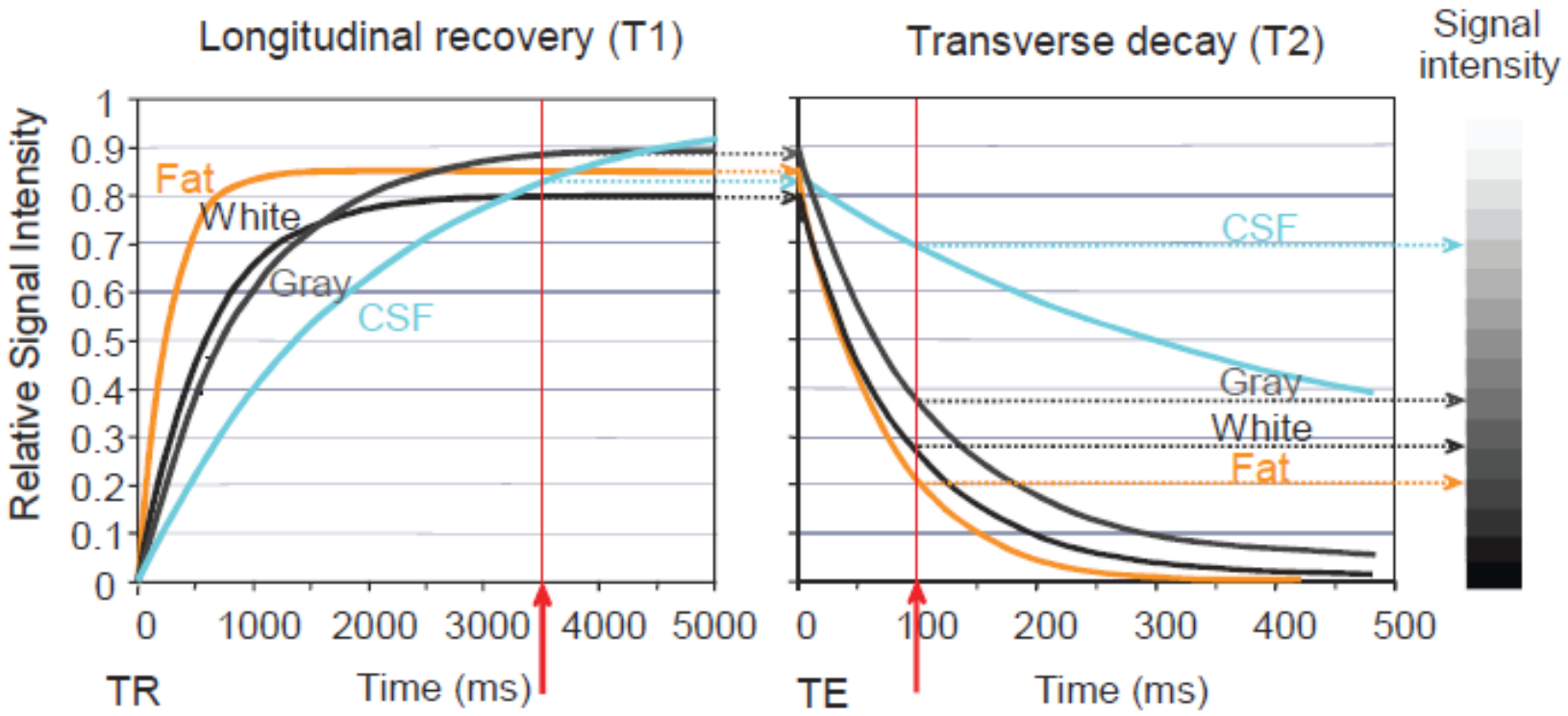

T2 weighted contrast requires the use of a long TR (e.g., greater than 2,000 ms) to reduce T1 influences, and a long TE (e.g., greater than 80 ms) to allow for T2 decay to evolve.
Compared to the proton density weighting, the difference is with longer TE.

Axial Images

T1 contrast weighting

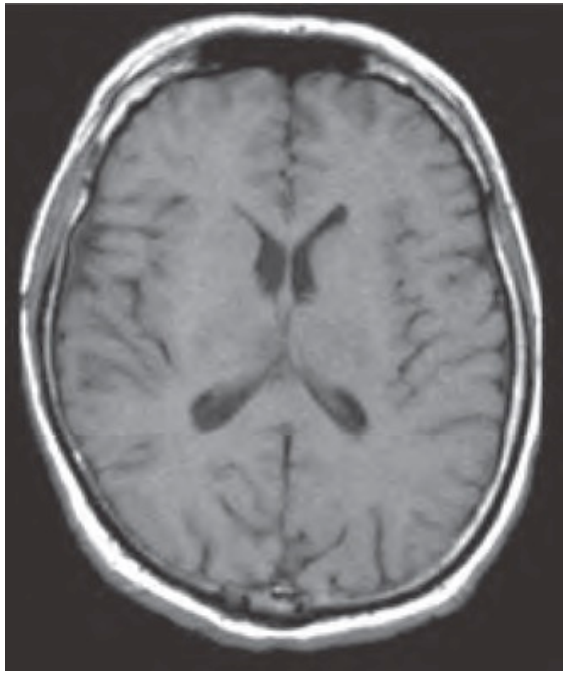

- Short T1 have high signal intensity (fat and white matter)
- Long T1 have low signal intensity (CSF).
- Short TE preserves the T1 tissue differences by not allowing significant T2 decay to occur.

Proton density contrast weighting

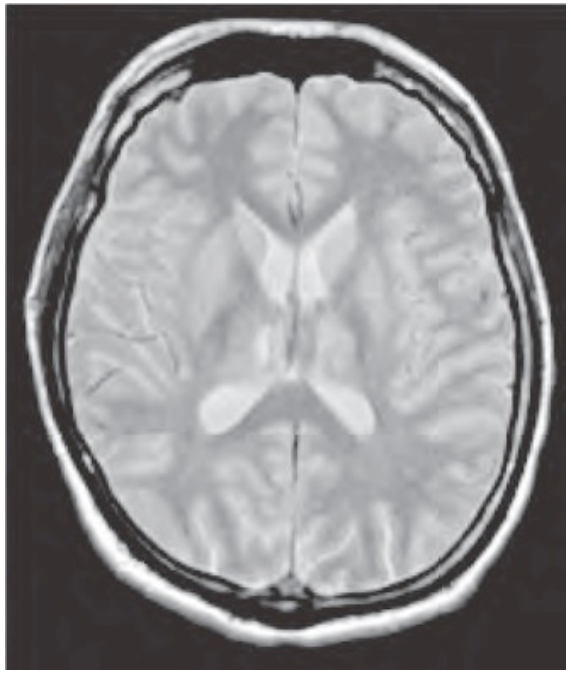

- Long TR minimizes T1 relaxation differences of the tissues.
- Signals with large proton density have higher signal intensity (CSF).
- Short TE preserves the proton density differences without allowing significant T2 decay.
- High SNR

T2 contrast weighting

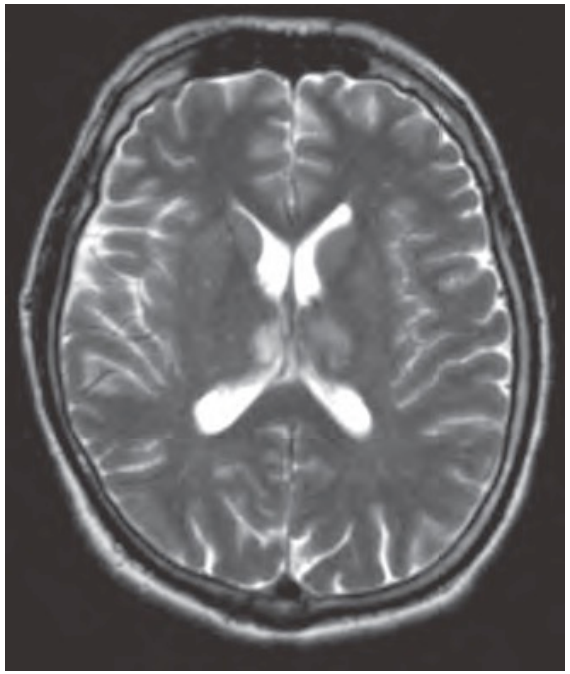

- Long TR minimizes T1 relaxation differences of the tissues.
- Long TE allows T2 decay differences to be manifested.
- This sequence has high contrast.

MR Signal Localization

Spatial localization is essential for creating MR images and determining the location of discrete sample volumes for MR spectroscopy.

This is achieved by superimposing linear magnetic field variations on the main (B_0) field to generate corresponding position-dependent variations in precessional frequency of the protons

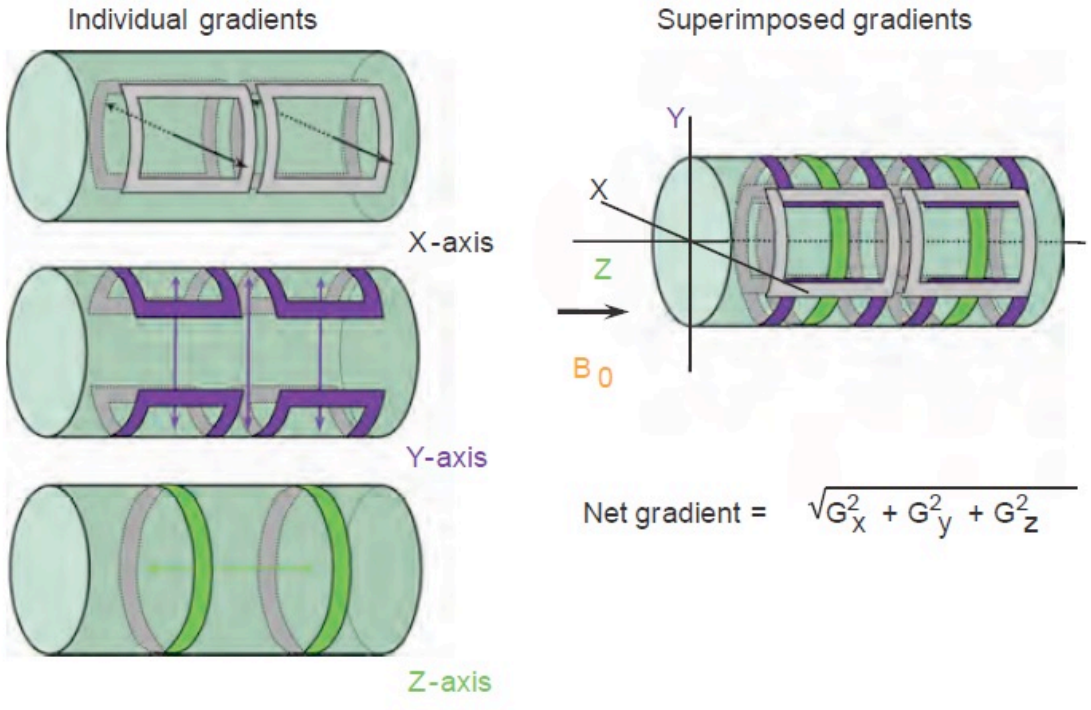

- Field gradients (G) (slice select, frequency encode, and phase encode) are produced by three separate coil pairs placed within the central core of the magnet, along the *x, y,* or *z* directions.

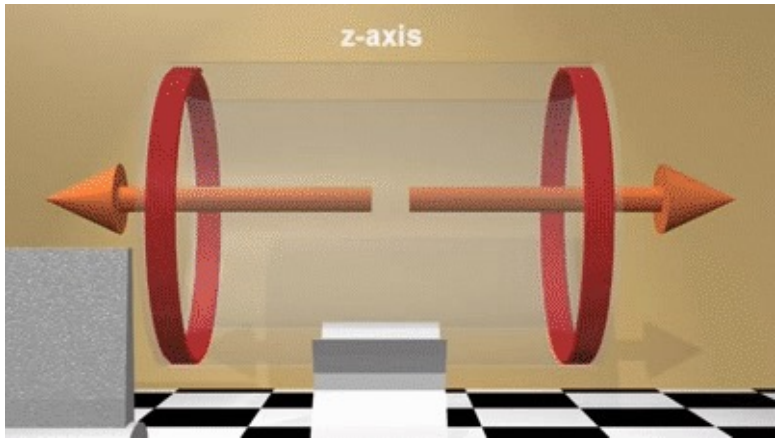

Slice Select Gradient - SSG

Localization of protons in the three-dimensional volume requires the application of three distinct gradients during the pulse sequence: slice select, frequency encode, and phase encode.

RF pulse, when turned on during the application of the **slice select gradient (SSG)**, determines the slice location of protons in the tissues that absorb energy

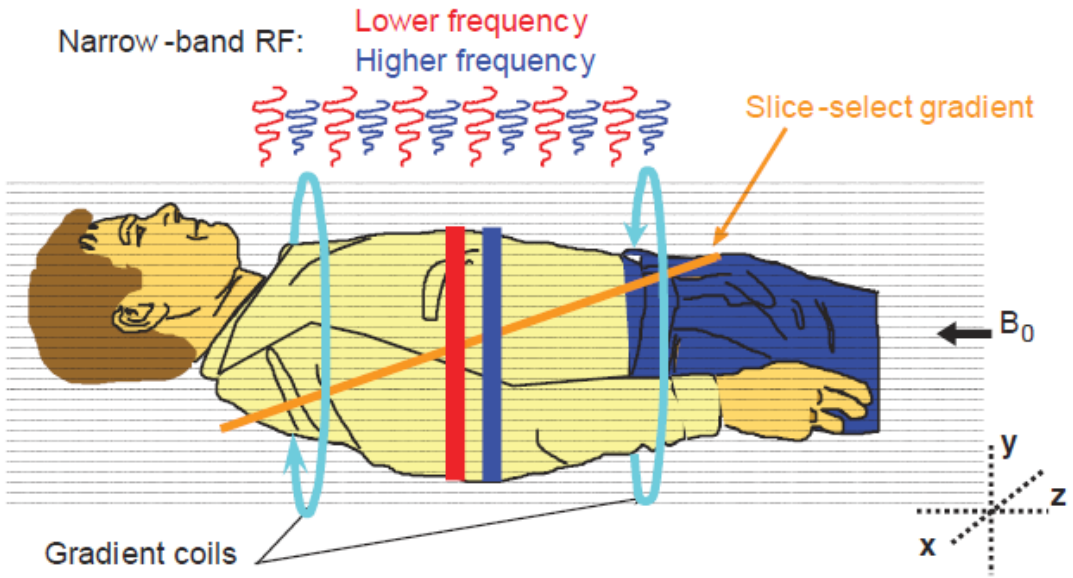

The *SSG* disperses the precessional frequencies of the protons in a known way along the gradient.
A narrow band RF pulse excites only a selected volume (slice) of tissues, determined by frequency, BW, and SSG strength.

Frequency Encode Gradient - FEG

The *FEG*, also known as the *readout gradient*, is applied in a direction perpendicular to the SSG, along the "logical" x-axis, during the evolution and decay of the induced echo.
Net changes in precessional frequencies are distributed symmetrically from 0 at the null to $+f_{max}$ and $-f_{max}$ at the edges of the FOV under the applied FEG.

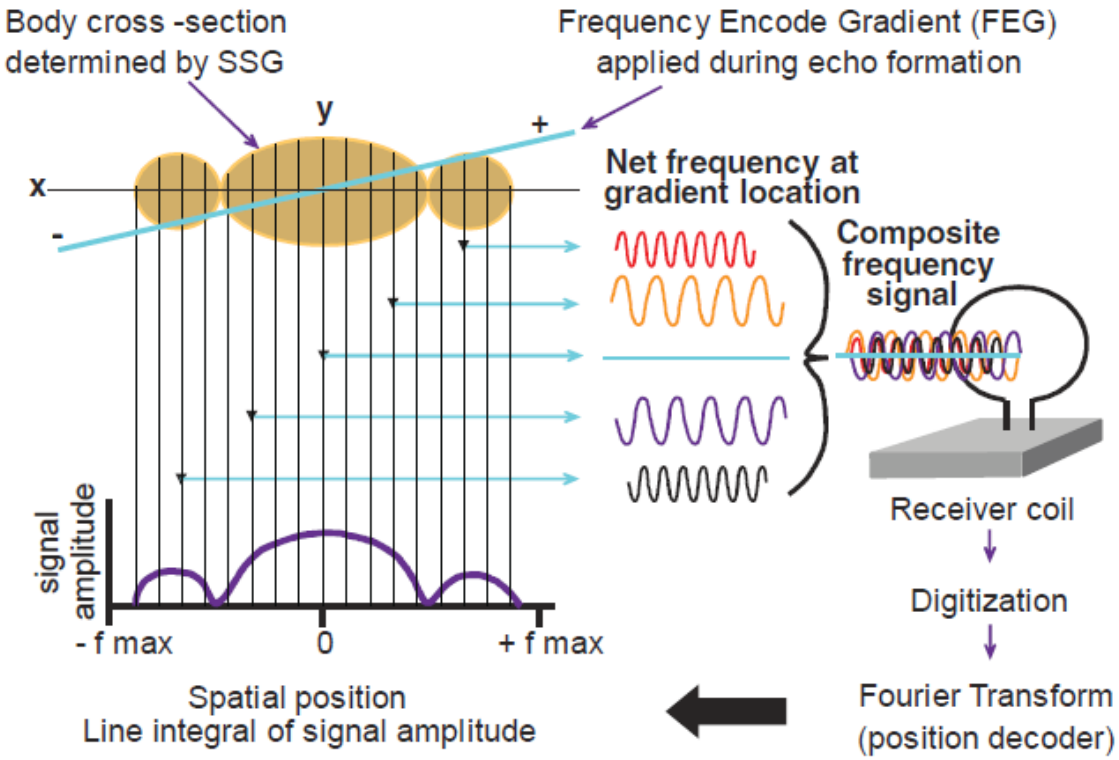

Phase Encode Gradient - PEG

Position of the protons in the third orthogonal dimension is determined with a PEG, which is applied after the SSG but before the FEG, along the third orthogonal axis.

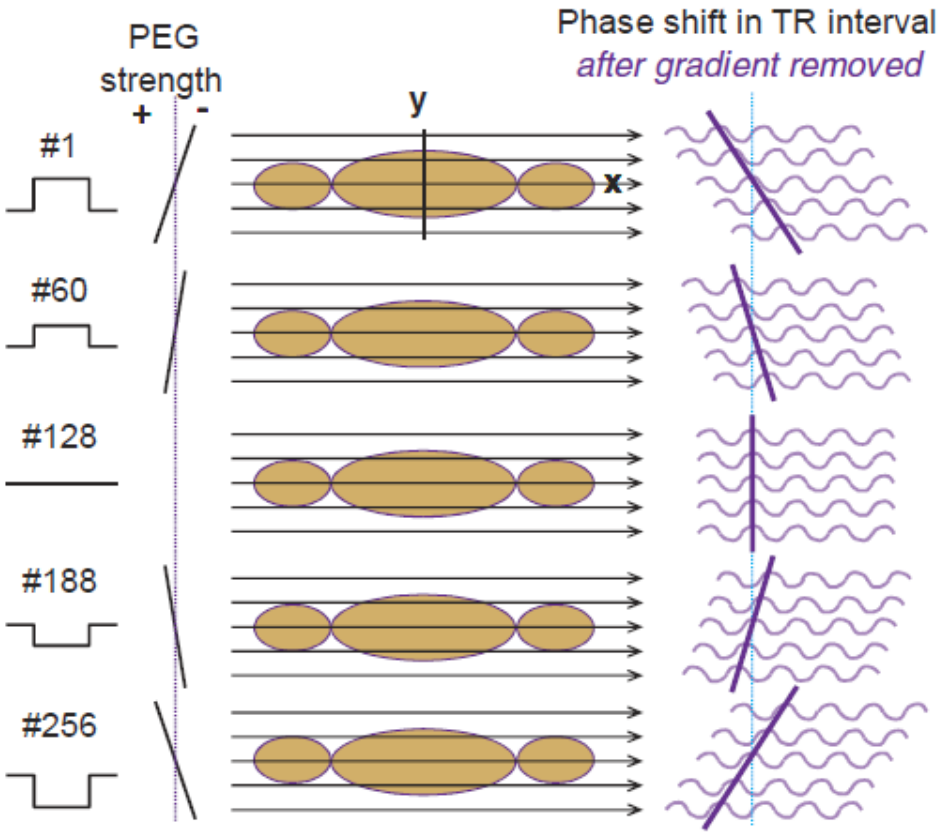

- The PEG is applied *before* the FEG and *after* the SSG.
- The PEG produces a spatially dependent variation in angular frequency of the excited spins for a brief duration, and generates a spatially dependent variation in phase when the spins return to the Larmor frequency.

Two-Dimensional Data Acquisition

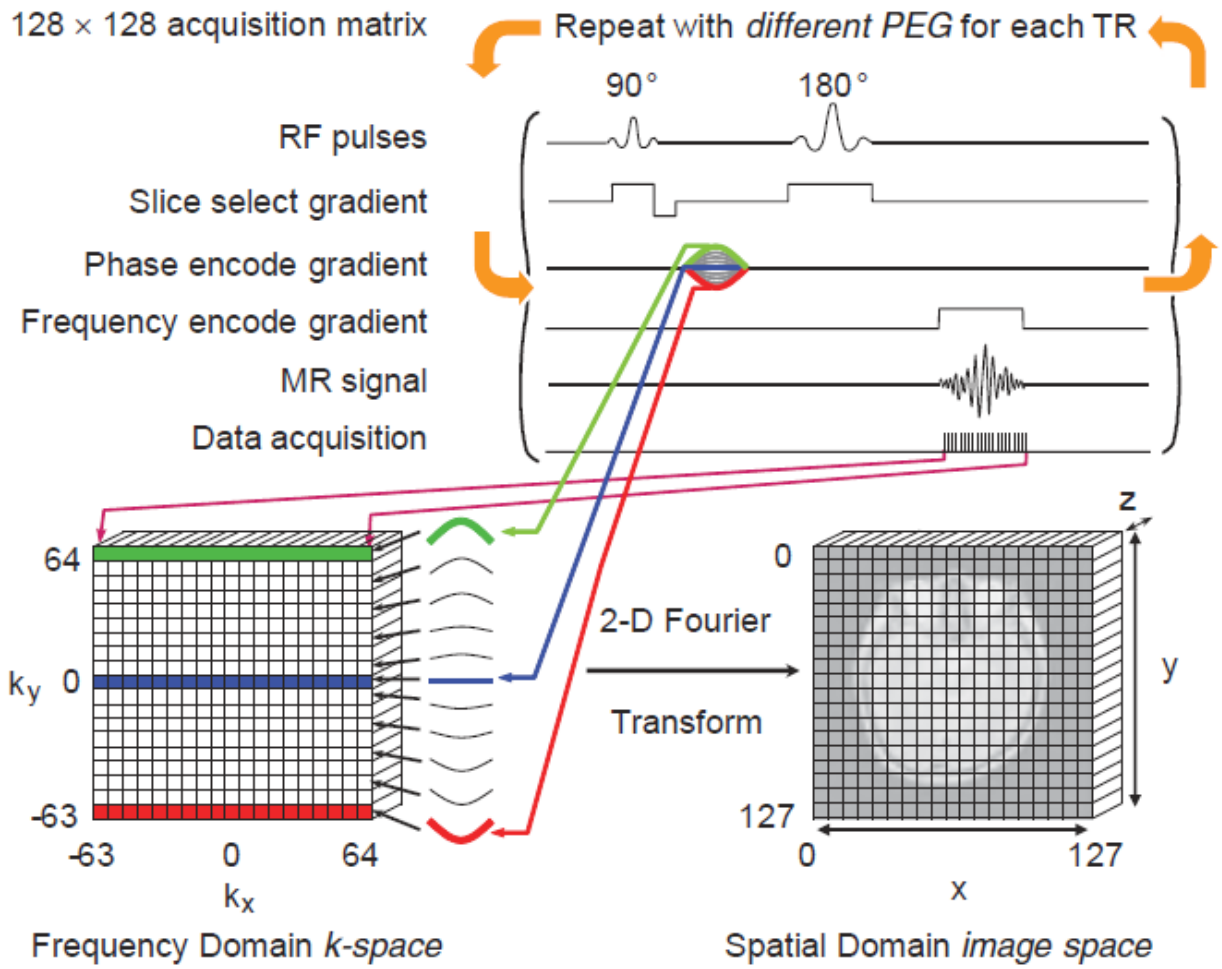

- MR data are acquired into k-space matrix, where each row in k-space represents spatially dependent frequency variations under a fixed FEG strength, and each column represents spatially dependent phase shift variations under an incrementally varied PEG strength.
- Data are placed in a specific row determined by the PEG strength for each TR interval.
- The grayscale image is constructed from the two-dimensional Fourier transformation of the k-space matrix by sequential application of one-dimensional transforms along each row, and then along each column of the intermediate transformed data.
- The output image matrix is arranged with the image coordinate pair, x = 0, y = 0 at the upper left of the image matrix.

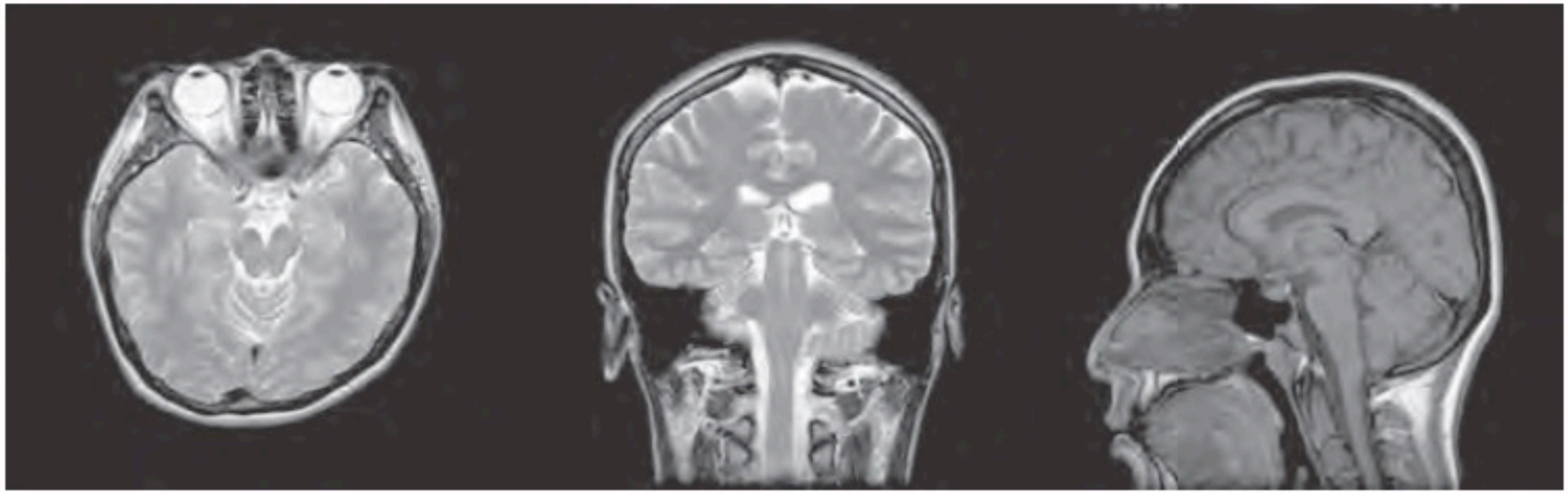

Axial Coronal Sagittal

Applications and challenges

- ❑ RMI for dosimetry redout
- ❑ Radiomics
- ❑ Nanoscale and microscale RMI

Dosimetry redout - Polymer gels

- Water: 80% - 90%
- Gelling substance: Agarose or Polyvinyl alcohol (PVA): 5% - 10%
- Monomers: 3% - 6%

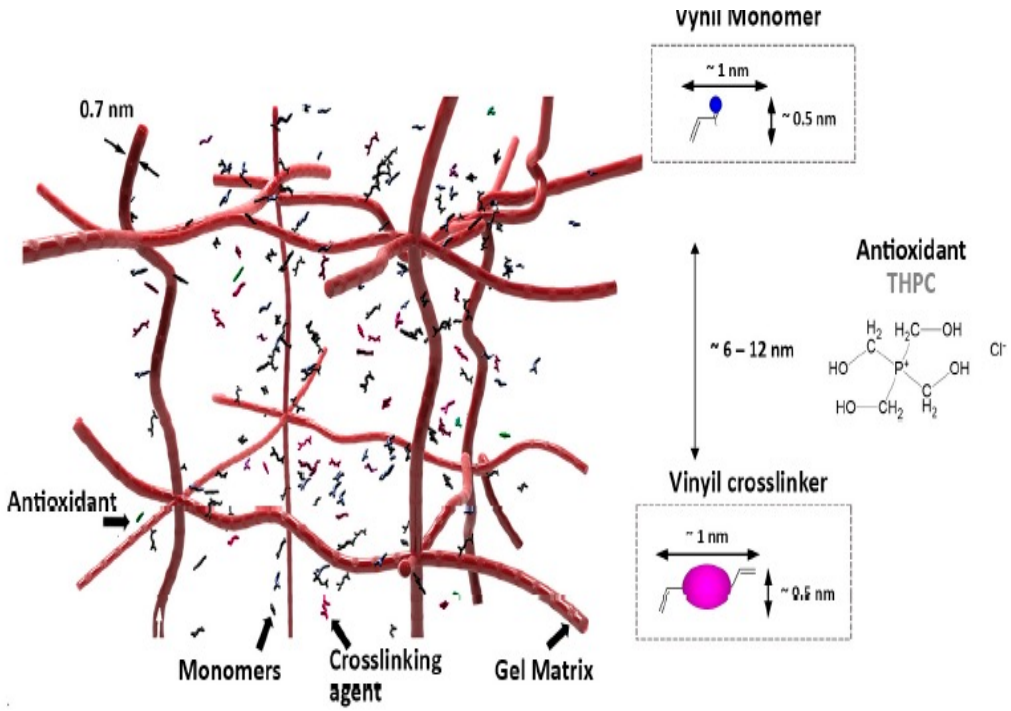

[1]

Detectors		
1D Ionization chambers	2D Radiochromic films	3D Gel dosimeters

Polymer gels

Chemical – physical principles

- Radiolysis ($10^{-15} - 10^{-14}\ s$): $H_2O \rightarrow 2R^{\cdot}$
- Recombination of reactive particles (local thermal equilibrium after $10^{-11}\ s$)
- Radical diffusion (main intermediates after $10^{-8}\ s$)
- Reaction with monomers
  - Initiation step: $R^{\cdot} + M_n \rightarrow RM_n^{\cdot}$
  - Propagation reaction: $RM_n^{\cdot} + M_m \rightarrow RM_{n+m}^{\cdot}$
  - The radical binds to the monomer and thus we have polymer growth

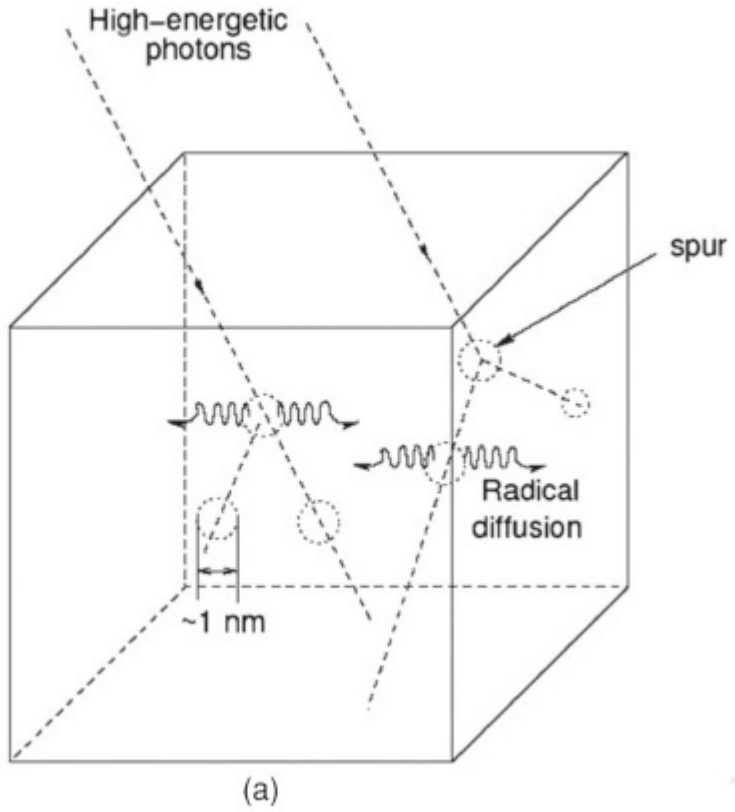

Amount of polymers proportional to the absorbed dose

End to End test – External Beam Radiotherapy

1) Polymer gel [4]

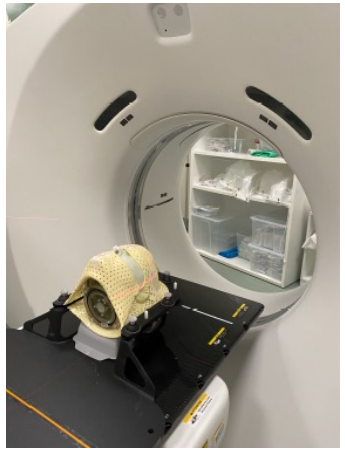

2) CT acquisition [6]

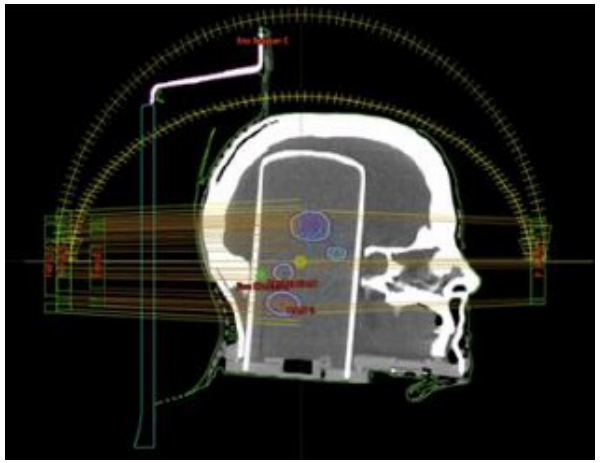

3) Creation of the verification plan [6]

4) Delivery of the verification plan [6]

5) MRI readout [6]

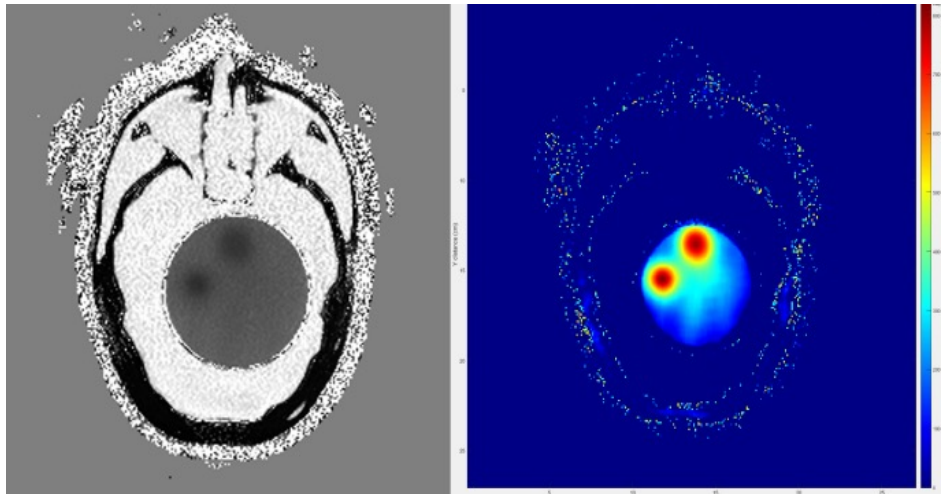

6) R_2 map and dose distribution (M4) [4]

Imaging – MRI Readout Methods

- Reduction of nearby water molecules mobility
- Decrease in spin-spin relaxation time T_2
- T_2 maps
- R_2 maps

$$R_2(i,j) = \frac{1}{\mathrm{TE}_2 - \mathrm{TE}_1} \ln \left| \frac{S_1(i,j)}{S_2(i,j)} \right|$$

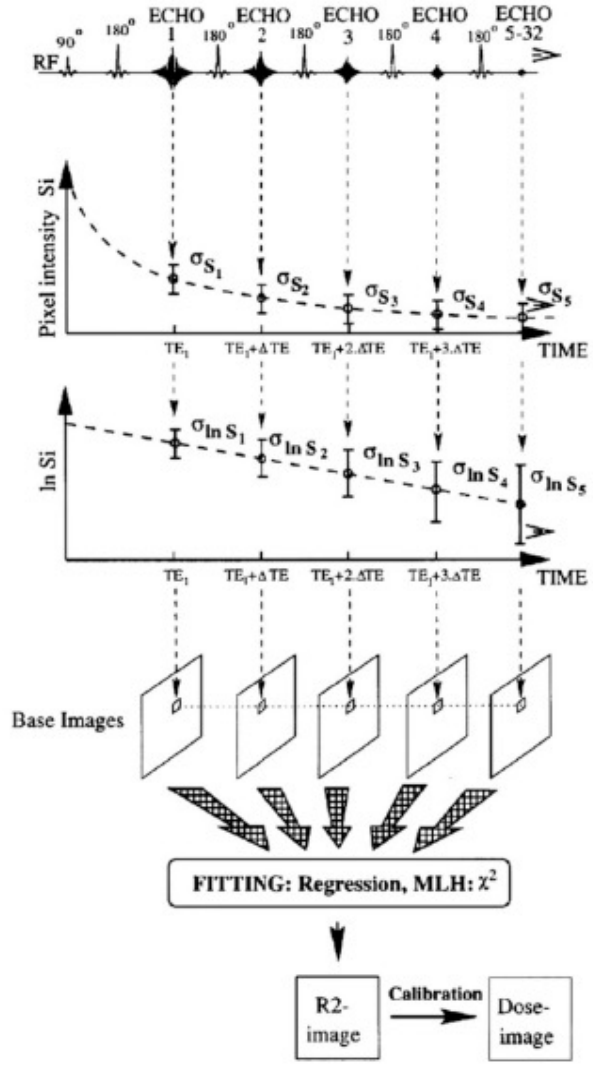

Dose comparison

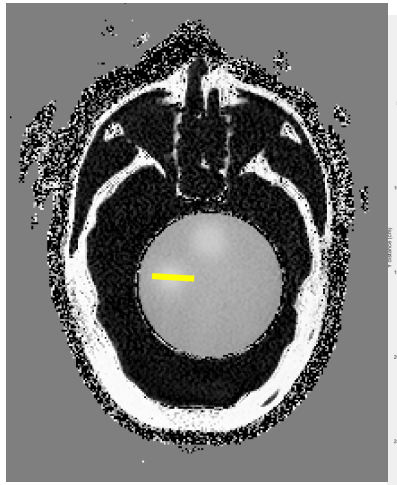

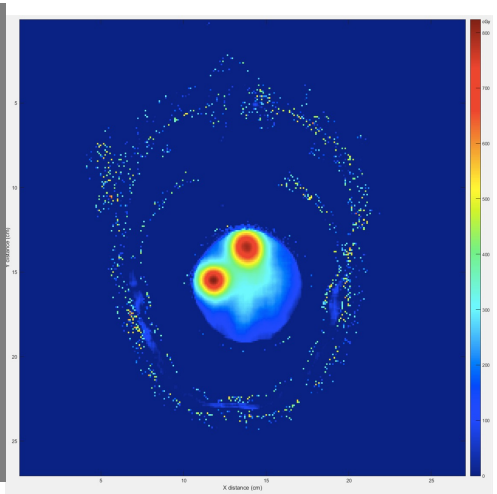

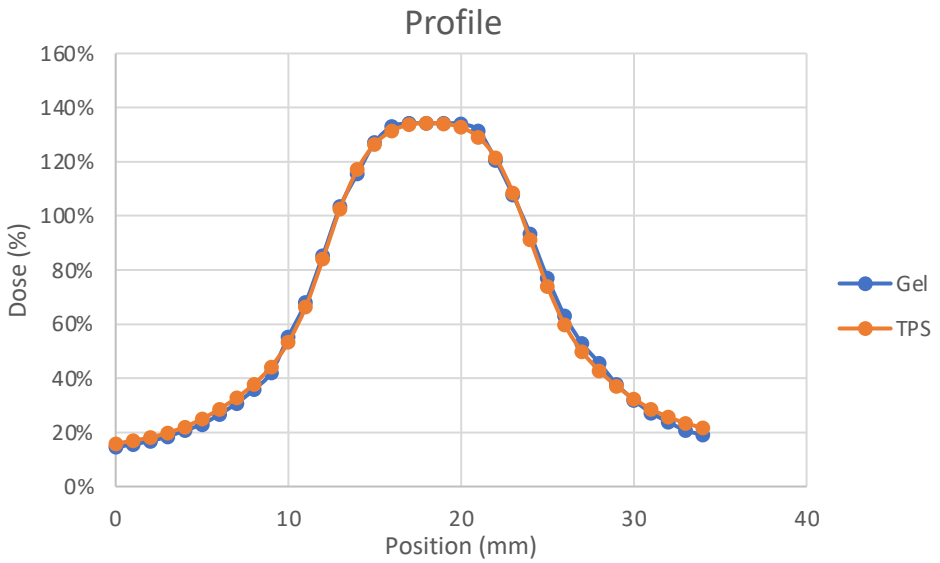

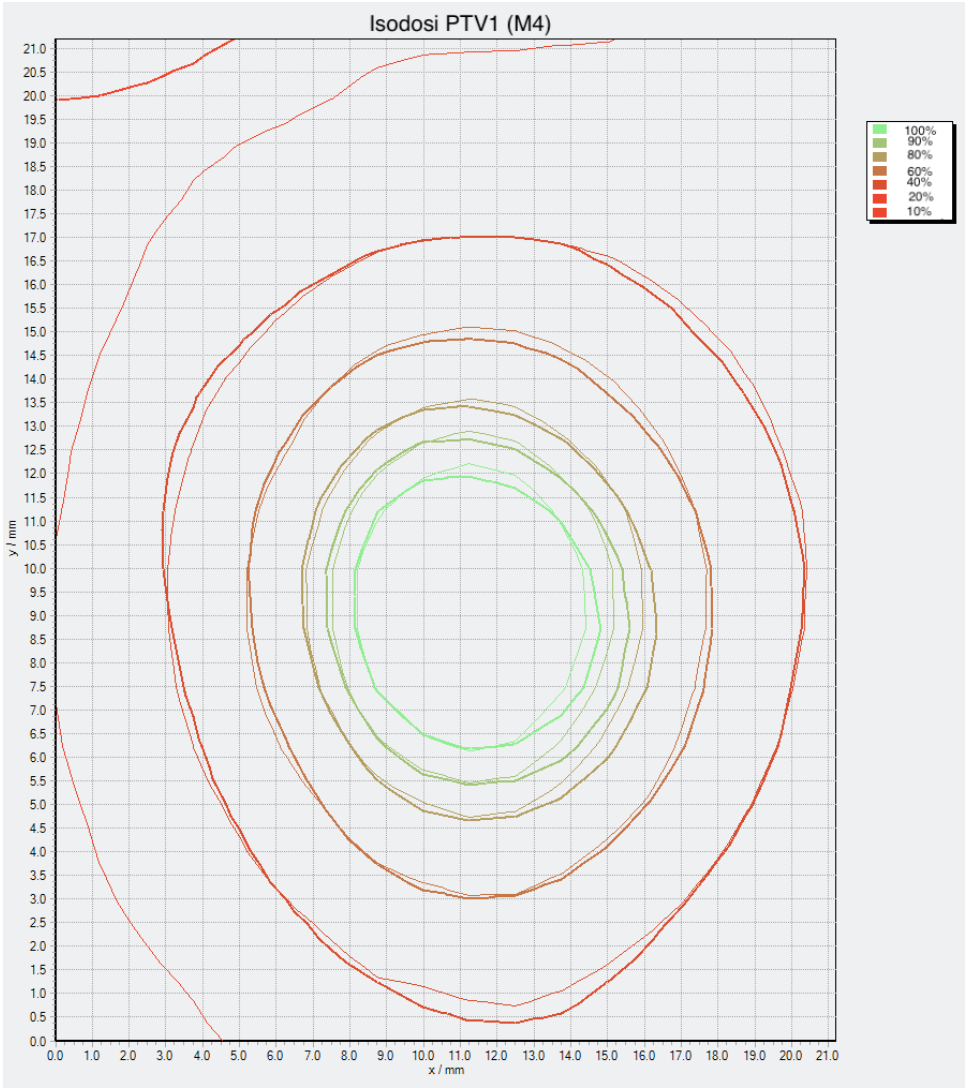

Radiomics

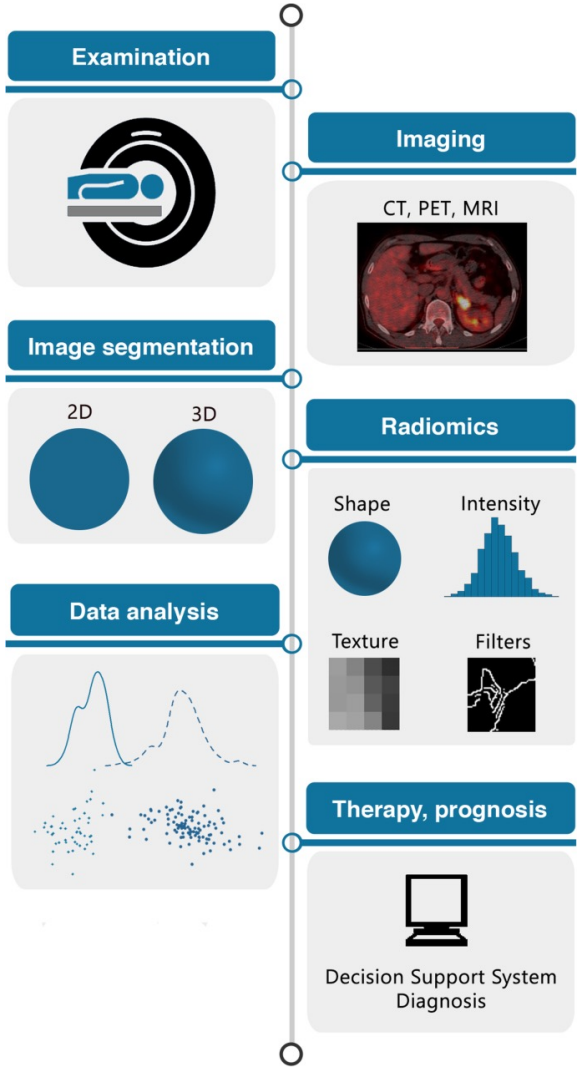

Radiomics: the extraction of quantitative information from clinical images and their correlation with the clinical outcome

Quantitative imaging allows to ask to some **prediction and classification tasks** and contributes, along with the other -omics sciences, to the **improvement of personalized medicine.**

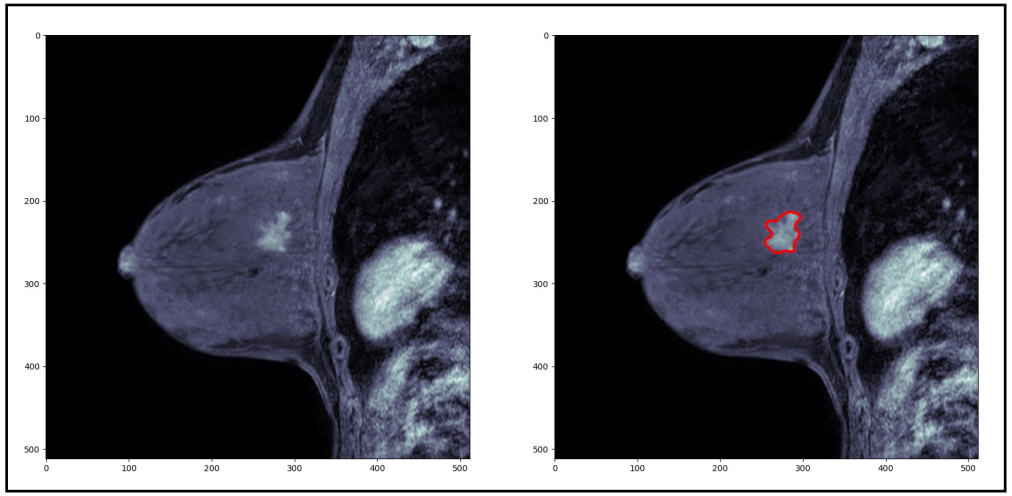

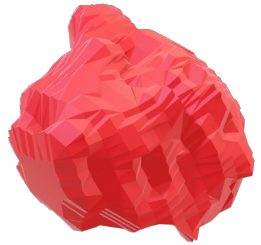

Prediction of pathological Complete Response (pCR) to Neoadjuvant Chemotherapy (NAC) in Breast Cancer

- pCR to NAC: the eradication of all invasive disease in the breast and axilla areas;
- Less than 10-50% of patients achieve the pCR; classification of patients who may or may not achieve pCR is crucial.

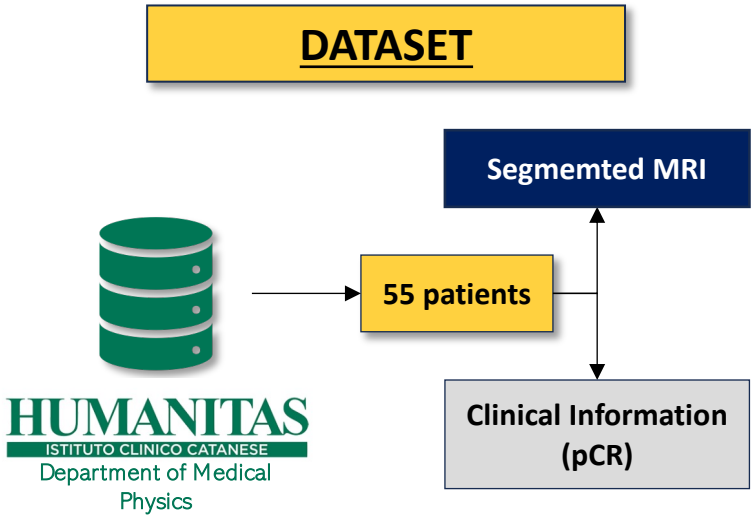

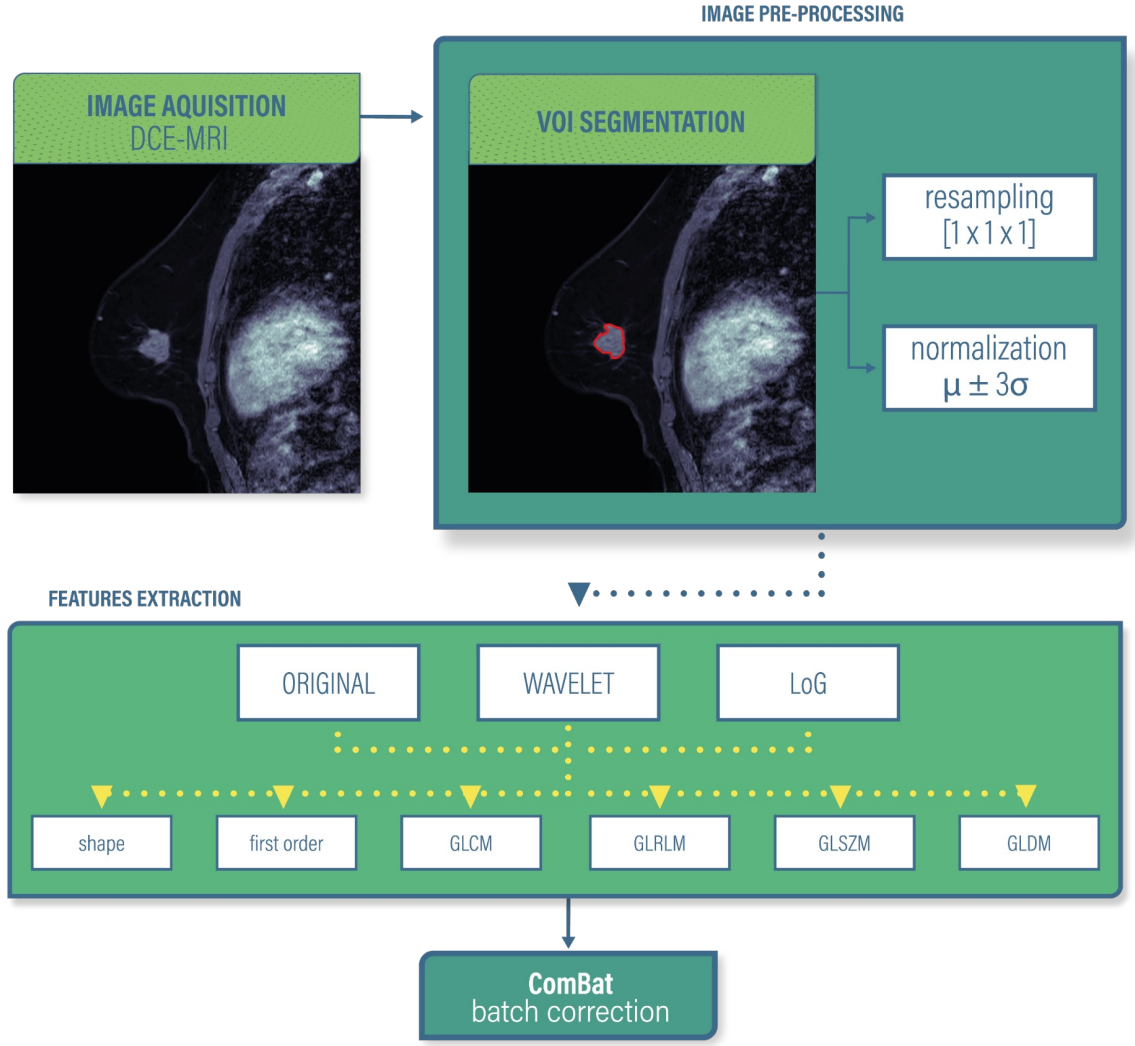

Nanoscale and microscale magnetic resonance imaging

Cell-to-cell heterogeneities have high biological relevance, for instance, in developing antibiotic resistance, carcinogenesis, and even immune responses.

Conventional NMR spectroscopy requires macroscopic sample volumes of up to several hundred microliters, impeding its use for single-cell analysis

These limitations can be overcome by a novel NMR sensor based on quantum defects in the diamond lattice

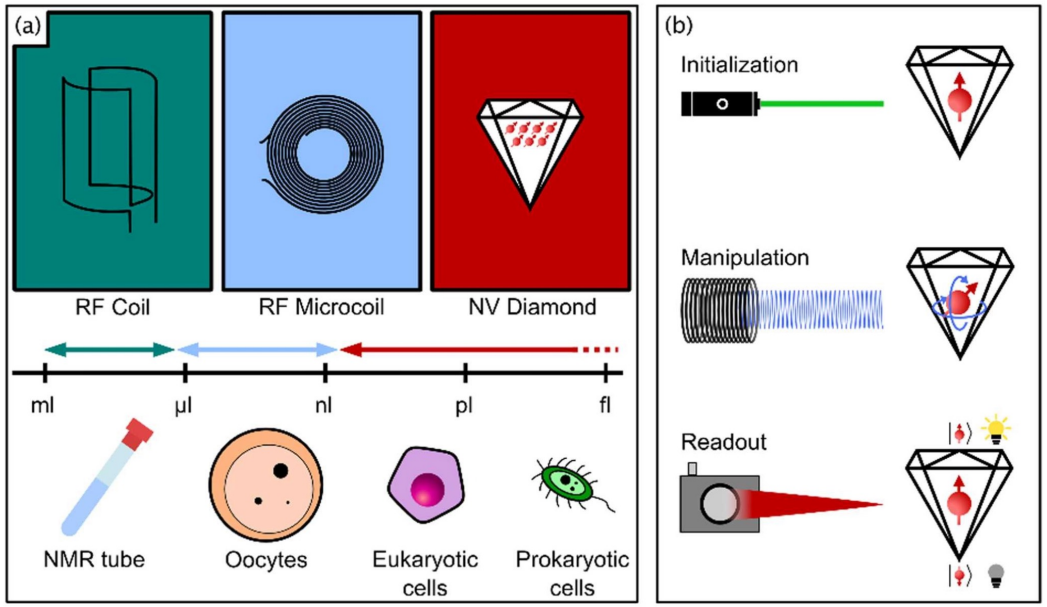

- The NV-spin state can be initialized optically by laser excitation,
- The NV-spin state can be coherently manipulated with resonant microwave (MW) fields, and I
- The NV-spin state can be read out optically by its spin-state-dependent fluorescence, which enables optically detected magnetic resonance experiments

Conclusions

- **Research needs many Marcello Baldo!**
- **Happy birthday Marcello**

Thank you for your attention